Cruz González, JM.; Fita Fernández, IC.; Soriano Martinez, L.; Paya Bernabeu, JJ.; Borrachero Rosado, MV. (2013). The use of electrical impedance spectroscopy for monitoring the hydration products of Portland cement mortars with high percentage of pozzolans. Cement and Concrete Research. 50:51-61. doi:10.1016/j.cemconres.2013.03.019.

MECHANICAL, MICROSTRUCTURAL AND ELECTRICAL PROPERTIES OF PORTLAND CEMENT MORTARS WITH HIGH REPLACEMENT BY POZZOLANS

J.M. Cruz[1], I.C. Fita[1*], L. Soriano[2], J. Payá[2], M.V. Borrachero[2]

[1] *Departamento de Física Aplicada, Universitat Politècnica de València. Camino de Vera, 46022 Valencia, Spain.*

[2] *ICITECH, Instituto de Ciencia y Tecnología del Hormigón, Universitat Politècnica de València.*

* corresponding author: Tel. 34 96 387 95 22, e-mail address: infifer@fis.upv.es

ABSTRACT

In this paper, mortars and pastes containing large replacement of pozzolan were studied by mechanical strength, thermogravimetric analysis (TGA), scanning electronic microscopy (SEM), mercury intrusion porosimetry (MIP) and electrical impedance spectroscopy (EIS). The effect of metakaolin (35 %) and fly ash (60 %) was evaluated and compared with an inert mineral addition (andalusite). The portlandite content was measured, finding that the pozzolanic reaction produced cementing systems with all portlandite fixed. The EIS measurements were analyzed by the equivalent

electrical circuit (EEC) method. An EEC with three branches in parallel was applied. The dc resistance was related to the degree of hydration and allowed us to characterize plain and blended mortars. A constant phase element (CPE) quantified the electrical properties of the hydration products located in the solid-solution interface and was useful to distinguish the role of inert and pozzolanic admixtures present in the cement matrix.

KEY WORDS: Electrical Properties (C), Pozzolan (D), Fly Ash (D), Metakaolin (D).

1. INTRODUCTION

Construction is an extremely dynamic industry field which continuously searches for new materials to improve the properties of concrete and the safety of its manufacture. The use of pozzolans has greatly improved the mechanical properties and durability of mortar [1]. In the future, a concrete without added pozzolanic or hydraulic materials (Supplementary cementing materials, SCM) will be the exception to the rule [2].

Pozzolans such as Fly Ash (FA) and Metakaolin (MK) are mineral admixtures that contain silica and/or alumina in a glassy state. Pozzolans

react with the calcium hydroxide produced from the hydration of the cement in the presence of water to form cementing hydrated products [3]. The reactivity of a pozzolan depends on its chemical and mineralogical composition, the type and proportion of active phases, the specific surface of the particles, the pozzolan/cement ratio, as well as the water/binder ratio, curing time and curing temperature [3-5].

FA is a waste product from coal-fired power plants, widely used as replacement material in Portland cement. Not only does FA increase the workability of cement pastes and mortar [6, 7] but it also improves their durability and their mechanical properties for long curing times [8, 9]. FA particles can accelerate the hydration reaction of cement through the filler effects [10, 11]. The pozzolanic reaction of FA is slow, so particles continue to react with the pore solution in the hydrated cement for years [10-13]. The proportion of FA in cementitious materials is usually determined by different engineering applications and different curing conditions. For instance, for reinforced and prestressed concrete, the FA content is limited to 22 and 35 % (by weight) according to the stipulated regulations [14]. For other uses and manufactured products special cements can be added up to 70 % in the binder.

MK is a pozzolan which is obtained synthetically by the calcination of kaolin at temperatures in the range of 700-850 °C [15]. It is a very fine

material that has shown to be an active pozzolan from the early ages of curing, producing significant improvements in the mechanical strength and durability of mortars [16]. Some advantages of using MK in mortars and concretes of Portland cement include the increase in mechanical strength, the decrease in permeability, the increased resistance to chemical attack, the reduced alkali-silica reaction (ASR), and the reduction in shrinkage. These advantages stem from the fact that their small particle size and pozzolanic reactivity change the porosity of the matrix, generally improving the durability of the concrete [17].

Products containing Portland cement such as cement paste, mortar and concrete are porous materials with a complex porous phase. Porosity is classified by size in two main groups: capillary porosity (> 20 nm) and gel porosity, furthermore, pores can be connected (open porosity) or not connected (closed porosity). The tortuosity of open porosity, the mean pore size and pore size distribution are properties that change during hydration reactions [18, 19].

Currently, no single method is available to measure the pore structure of cement composites. The most widely used methods are mercury intrusion porosimetry (MIP) and adsorption-desorption of nitrogen (NAD). The MIP measurement appears to be the preferred method for assessing pore structure, due to its wide range of pore size measurements, although

sometimes this measurement loses accuracy due to the induction of microcracks by the high pressure in the intrusion and the proportion of "ink-bottle" pores [20]. The NAD has also been used to determine the pore structure of cement-based materials [21]. A recent work [22] studied the porous structure of cement pastes incorporating large quantities of FA by using MIP and NAD techniques and relating pore structure to the hydration process. The inclusion of MK as a cement replacement greatly improves the pore structure of concrete. The total porosity decreased substantially and there was a considerable reduction in the mean (or median) pore diameter of the samples with increasing amounts of MK until 20 % of replacement [23].

A non-destructive method recently used to assess the pozzolanic effects in the microstructure of cement mortar is electrical impedance spectroscopy (EIS) [24, 25]. The electrical properties of saturated porous materials with low and medium frequency, from a few Hz to 1 MHz, reflect the movement of ions in the pore solution and are related to the micro-geometry of pore structure. The dc electrical resistivity is proportional to the mobility of ions in the bulk of the solution of the connected porosity. The formation factor and the diffusion, both related to the porosity, can be calculated from the resistivity of the material and the resistivity of the pore solution [26]. The electrical capacity of the material is related to the geometry of the blocked pores [27] and with its fractal character [28]. Unlike MIP and NAD methods, EIS measurements are advantageous because they are non-

destructive and can be performed quickly and automatically at any time during the hydration reaction. Also they can characterize the degree of hydration of Portland cement mortar at early ages, complementing measurements of mechanical properties.

The aim of this research is to analyze mortars containing large amounts of pozzolan since they can consume virtually all of the portlandite released by the cement hydration. To this end, a high-reactive pozzolan, such as MK (35 % replacement), and other less active pozzolans such as FA, but with a higher replacement percentage (60 % replacement) were used. The effect of pozzolans in the mortars was evaluated by using an inert mineral addition of andalusite (AN) in the same replacement quantities for comparison. Firstly (sections 3.1 and 3.2), mechanical strength and consumption of portlandite by means of thermogravimetric analysis (TGA) were measured at different ages. Secondly (sections 3.3 and 3.4), the microstructure was analyzed by scanning electron microscopy (SEM) and MIP. And finally (section 3.5), EIS measurements were analyzed by the equivalent electrical circuit (EEC) method. The obtained electrical parameters were compared with the others measurements in order to assess the evolution of the microstructure using this non-destructive technique.

2. MATERIALS AND METHODS

2.1. Materials

For all mixtures (pastes and mortar) an ordinary Portland cement (OPC) was used (spanish Portland cement: CEM I 42.5 R supplied by the company Asland Lafarge). The mineral additions were 1) MK from the ECC International Company, commercialized under the name of MetaStar, 2) FA from the Thermoelectric power plant in Andorra (Teruel-Spain) and 3) an inert (or filler) aluminosilicate (andalusite, Al_2SiO_5) (AN) supplied by Sibelco. Also for the manufacture of mortars, siliceous sand with fineness modulus of 4.1 was used. The chemical composition and the mean particle diameter (D_m) of the cement (CEM) and the mineral additions are given in Table 1.

Table 1.

Chemical composition (% by weight) and mean particle diameter (D_m) of mineral additions and the cement used.

	SiO_2	Al_2O_3	Fe_2O_3	CaO	MgO	SO_3	K_2O	Na_2O	L.O.I.*	D_m(μm)
MK	52.10	11.00	4.32	0.07	0.19	-	0.63	0.26	0.60	5.84
FA	38.85	24.52	19.63	10.52	1.20	0.47	1.17	0.22	1.56	29.78
AN	42.88	51.09	1.18	1.54	0.57	0.79	0.66	0.37	0.92	31.05
CEM	20.21	4.94	2.85	62.87	1.05	3.54	0.92	0.10	3.02	25.49

**Loss on ignition*

The granulometric curves of these materials are plotted in Fig. 1. The shapes of particle size distribution of FA and AN are relatively similar with the same D_m value of 30-31 µm. For MK the curve is different and D_m is five times lower.

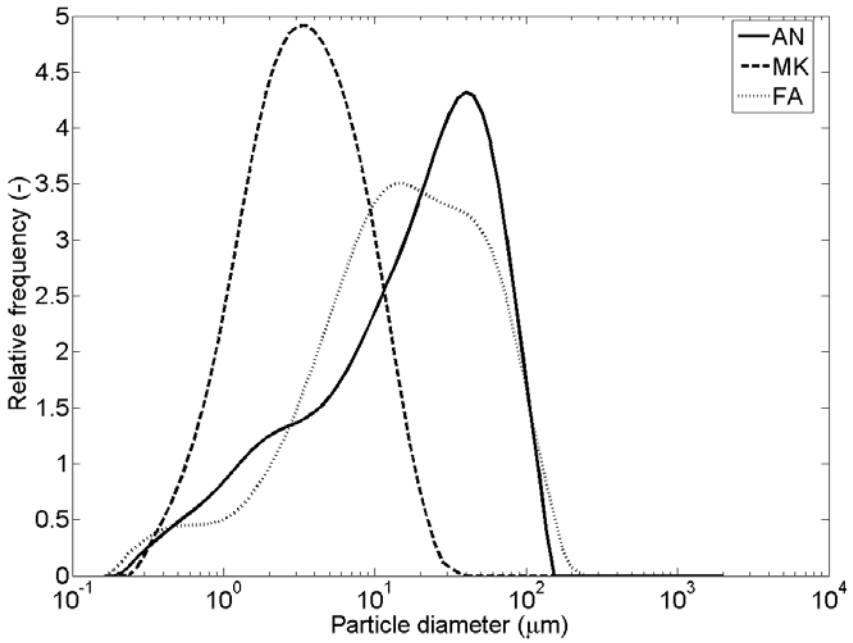

Fig. 1. Particle size distribution of mineral additions (relative frequency is measured in % by volume).

2.2. Methods

For studies of electrical measurements and mechanical strength, mortars were prepared with a standard water/binder (w/b) ratio of 0.5 and an aggregate/binder ratio equal to 3 (UNE-EN 197-1). The composition of mortars is detailed in Table 2.

Table 2.

Mixture composition for mortars.

Mortar	Cement (g)	Water (g)	Addition (xx) (g)	Replacement (% w)	Sand (g)
m-OPC	450.0	225.0	--	--	1350.0
m-35AN	292.5	225.0	(AN) 157.5	35	1350.0
m-35MK	292.5	225.0	(MK) 157.5	35	1350.0
m-60AN	180.0	225.0	(AN) 270.0	60	1350.0
m-60FA	180.0	225.0	(FA) 270.0	60	1350.0

Prismatic mortar specimens of 25.4 x 25.4 x 280 mm^3 were prepared; after reaching the age for testing (3, 7, 15, 28 and 180 days of curing), 4 cubes of 25.4 x 25.4 x 25.4 mm^3 were cut from each specimen and tested to compressive failure. Mechanical measurements were performed on an Instron Model 3382 universal machine, with the charge rate set at 1 mm/min.

For thermogravimetric studies, pastes were prepared with a 0.5 w/b ratio, and percentage replacement of cement by additions were of 35 or 60 % using the same proportion as in mortars (see Table 2). Samples were stored at 20 ºC and 100 % RH and curing ages were 1, 2, 3, 7, 15, 21, 28, 60, 90 and 180 days. For each selected curing age, pieces of the sample were ground and the hydration process was stopped by inmersion in acetone. Subsequently, the mixture was filtered, dried in a furnace at 60 ºC for 30 minutes and analyzed instantly in a 850 TGA Mettler-Toledo thermobalance. Heating range was 35-600 °C at a heating rate of 10 °C/min, with a continuous 75 mL/min flow of N_2. Aluminum crucibles with a pinhole lid were used and then sealed with the aim of achieving a self-generated water vapor atmosphere.

Pastes were characterized by SEM using a JEOL JSM6300 equipment to complete the microstructural study. To increase electrical conductivity, the samples were coated with gold by using BALTEC SCD 005 equipment. The conditions of the coating process are: exposure time of 90 seconds, intensity of 40 mA, working distance of 5 mm and pressure of $2.4 \cdot 10^{-2}$ mbar. The microanalysis was performed using OXFORD INSTRUMENTS Link-Isis system.

The pore size distribution of mortar specimens after 360 days of curing was determined through MIP using an AutoPore IV 9500 from Micromeritics

Instrument Corporation with an intrusion pressure between 13782 Pa and 227.4 MPa (size pore between 5.5 nm and 361 μm, according to Washburn relation).

The electrical impedance measurements were performed with the impedance meter HP-4284 A in the frequency range 20 Hz - 1 MHz. Four samples of each type of mortar were measured at the ages: 1, 2, 3, 7, 15, 21, 28, 57, 64, 92 and 210 days for m-OPC, m-35MK and m-60FA, and at the ages: 1, 2, 3, 7, 15, 21, 29, 66 and 99 days for m-35AN and m-60AN. The measuring cell consisted of two flat stainless steel electrodes of 25 x 70 mm^2 separated by 65 mm in length. A 25 x 25 x 160 mm^3 prismatic sample was introduced into the center of the cell, leaving two prismatic gaps of 20 x 25 x 70 mm^3 between the sample and the electrode. These gaps between the sample and the electrodes were filled with the lime saturated solution which was in equilibrium with the samples. In order to minimize any electrochemical effects, a minimum constant electric current of 100 μA was applied. Impedance (Z_m) was measured at four different heights of solution in the gap: h = 1.5, 3, 4.5, 6 cm. Admittance ($Y_m = 1 / Z_m$) was calculated and adjustments of real part [Re (Y_m)] and imaginary part [Im (Y_m)] against height (h) were performed. The applied procedure [25] is based on: using a variable area of measurement and analyzing Y_m versus h. It allows us to separate the admittance independent of height (Y_o) and the admittance proportional to height of the sample (Y_c). Y_o is related to cables, connectors and the edge effect of the prismatic sample in its lower and upper ends. The

corrected impedance ($Z_c = 1 / Y_c$) include only the intrinsic impedance of the mortar and the impedance corresponding to the solution and the cell electrodes in series. A free computer program (LEVM) was applied to Z_c for adjustment to an EEC. The EEC allowed us to separate two impedances in series included in Z_c.

3. RESULTS AND DISCUSSION

3.1 Mechanical strength

Changes in mechanical strength over time were studied by comparing the behaviors of pozzolanic materials and the inert addition. In Fig. 2 (a), the results until 180 days of curing are given with the mean compressive strength and its error bars, both were calculated from the four cubes tested. The compressive strength values for m-OPC and m-35MK were higher than for the other mortars, being m-35MK the mortar with the highest strength for all curing ages. As expected, the replacement of cement by 35 and 60 % of AN (m-35AN and m-60AN mortars) produced a significant decrease in the strength values of mortars. This addition was performed to observe the dilution effect when part of the cement was replaced by an inert mineral admixture. Using FA to replace 60 % of the cement, m-60FA, resulted in higher strength than mortars with AN in the same proportion, m-60AN, but

their values were much lower than m-OPC values. This result was expected since it is known that the pozzolanic effect develops more slowly for a FA than for other pozzolans such as MK. In the literature, it has been shown that for mortars with large FA replacements, the best results are obtained at longer curing ages, over 28 days [29].

In order to illustrate the pozzolanic effect of the addition, the strength activity index (SAI) values are plotted in Fig. 2 (b). This index was calculated according to the following expression:

$SAI = \sigma_{add}/\sigma_{opc}$

being σ_{add} and σ_{opc} the compressive strength for mortar with addition and m-OPC, respectively.

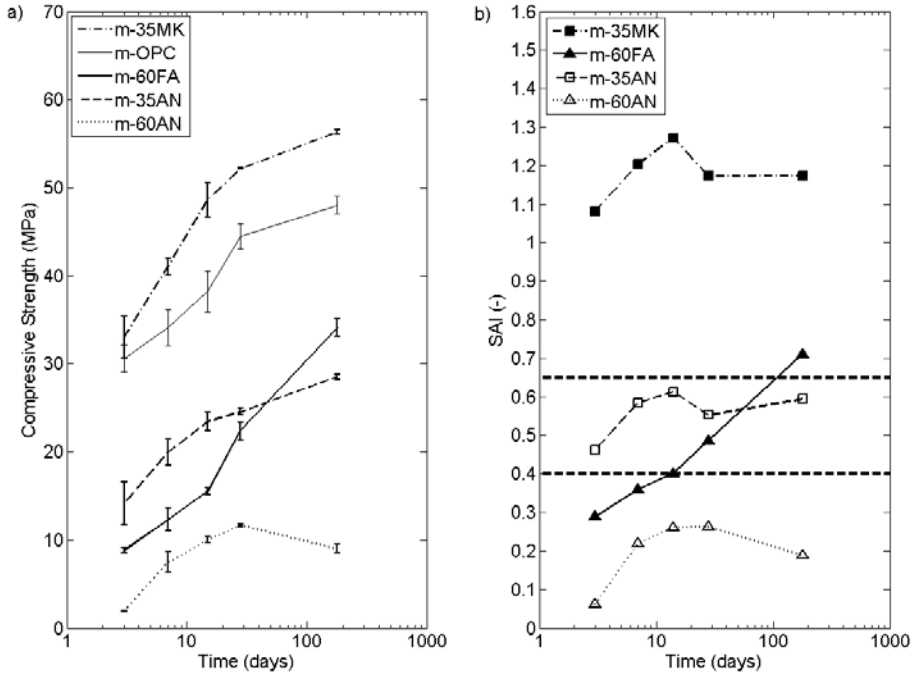

Fig. 2. a) Compressive strength values versus curing time for all mortars; b) SAI values of mortars versus curing time (3, 7, 15, 28, 180 days, in log scale).

The effects of inert and pozzolanic additions can be deduced from Fig. 2 (b). For the replacement 35 %, it becomes clear that m-35AN had a SAI slightly lower than 0.65, which corresponds to a mortar with 65 % cement, since there was a particle effect of the inert addition and the w/c ratio was higher than m-OPC. Mortar m-35MK had a SAI factor greater than one and also exceeded the value of 1.2 from the first days, demonstrating the high and early pozzolanic reactivity. Mortar m-60AN had a SAI about 0.2, when it should have had a SAI of about 0.4 if we consider its 40 % cement content, as we did for m-35AN. This could be because the amount of

cement in the binder was very low and, therefore, the w/c ratio of the material was very high; hence, the particle effect on mechanical properties was masked by the dilution effect. It is possible to evaluate the particle effect, especially when comparing m-60AN with m-60FA, because both additions had a similar particle size. The SAI value for m-60FA at early ages (3 or 7 days) was higher than that found for inert addition (m-60AN), highlighting the differences in the activation of the cement hydration by both types of additions. For longer curing times, the dilution effect in the mortar was compensated by the pozzolanic reaction and m-60FA presented a SAI value higher than 0.4 at 28 days, suggesting a notable effect of the reaction of FA particles in the development of strength. Mortar m-60FA reached values higher than 0.65 at 180 days of curing, illustrating the pozzolanic activity of this material. In this case, as the pozzolanic reaction of FA was slow, the SAI values increased continuously with curing time.

3.2 Thermogravimetric analysis (TGA)

Thermogravimetry studies were conducted to analyze the evolution of the pozzolanic reaction in terms of portlandite fixation. Tests were carried out at 1, 2, 3, 7, 15, 21 and 28 days of curing for pastes p-OPC, p-35AN and p-60AN. Pastes p-OPC, p-35MK and p-60FA were also tested at 60, 90 and 180 days of curing. Derivative Thermogravimetry (DTG) curves of OPC pastes and blended pastes at 28 and at 180 days are shown in Fig. 3

(a) and (b), respectively. The pozzolanic reaction increased the hydration products present in the cement paste, such as hydrated calcium silicates and hydrated calcium aluminosilicates (100-300 ºC interval of the DTG curves). For pastes cured at 28 days, the peak above 200 °C, which results from the combined water loss from hydrated calcium aluminosilicates, was more developed for pastes with pozzolans. Also p-35MK was the only paste that did not show a dehydroxylation of portlandite peak. At 180 days of curing, there was no portlandite present in p-60FA, and the peak related to the dehydration of calcium aluminosilicates was more pronounced than that found for the paste cured for 28 days.

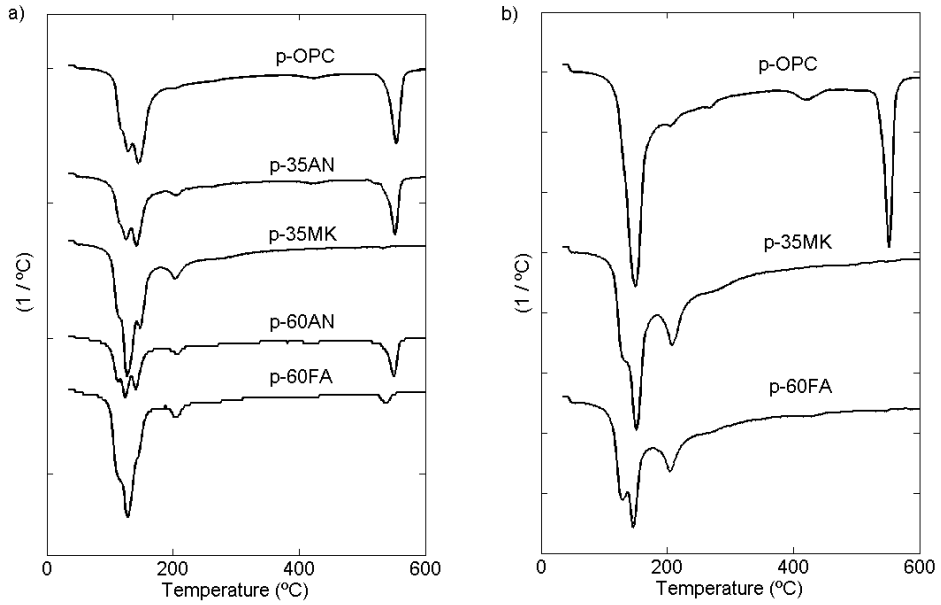

Fig. 3. DTG curves for pastes cured at 28 days (a) and 180 days (b). (The curves are separated in order to better observe the peak values)

The total weight loss (W_T, % in weight) was calculated as the weight loss measured from the thermogram curve (not shown) in the temperature range 35-600 °C. The portlandite content (CH) was calculated from the weight loss measured at the temperature range 500-550 °C (W_{CH}, % in weight) which is due to the dehydroxylation process of the portlandite:

$Ca(OH)_2 \rightarrow CaO + H_2O$

The percentage of portlandite content was calculated with the following expression:

$CH = [M(Ca(OH)_2/M(H_2O] \cdot W_{CH}$

where M is the molar mass.

The percentage of water associated with hydrates phases (H) was calculated as:

$H=W_T - W_{CH}$

Table 3 provides the values of CH and H for the different pastes at the tested curing ages.

Table 3.

Thermogravimetric data (% in weight) CH and H for OPC and blended pastes. (nd, not determined)

Pastes	p-OPC		p-35MK		p-35AN		p-60FA		p-60AN	
Time (days)	H	CH	H	CH	H	CH	H	CH	H	CH
1	12.90	7.40	8.8	0.60	7.9	5.4	5.4	2.80	5.4	3.4
2	15.30	9.90	12.3	3.80	10.8	6.6	7.5	3.60	6.9	3.9
3	15.90	8.40	14.5	0.02	13.2	6.9	8.5	3.30	7.2	4.4
7	14.90	10.50	14.9	0.00	10.8	8.3	8.9	2.90	7.6	4.6
15	21.10	11.00	20.9	1.20	17.3	8.1	13.5	2.70	12.3	4.5
21	17.80	11.10	17.7	1.30	12.8	8.4	12.7	1.40	11.0	4.7
28	18.70	11.80	20.9	0.00	13.7	8.5	16.6	1.40	10.3	5.3
60	20.90	12.00	22.3	0.00	nd	nd	17.2	1.20	nd	nd
90	17.90	11.70	18.8	0.00	nd	nd	13.8	0.00	nd	nd
180	17.70	10.80	17.9	0.00	nd	nd	13.5	0.00	nd	nd

Percentage of portlandite fixation (%CH) was calculated for all curing ages, taking into account the percentage of cement replacement for each paste and using the expression [30]:

$$\%CH = \frac{CH_O \cdot C - CH_P}{CH_O \cdot C} \cdot 100$$

where CH_O is the percentage of portlandite content in p-OPC for a given curing time; CH_P is the percentage of portlandite content in the pozzolan paste at the same curing age, and C is the proportion of cement present in the pozzolan paste (in per unit). Percentages of portlandite fixation for blended pastes are shown in Fig. 4.

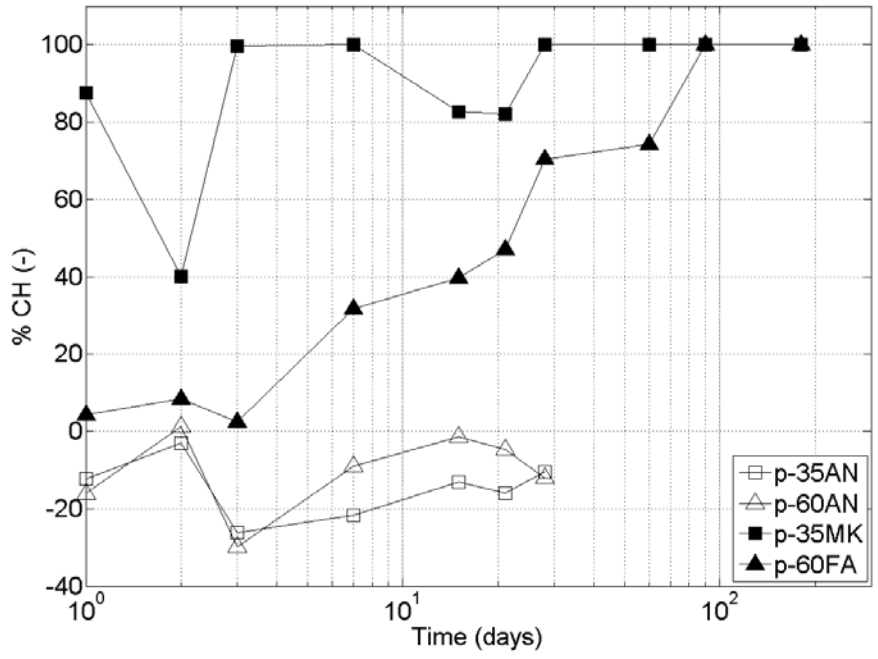

Fig. 4. Percentage of portlandite fixation versus curing time (log scale) for cement pastes with mineral additions.

All pastes with an inert addition presented negative values for fixation of portlandite, because the AN only acts as an inert filler, and this addition does not have a pozzolanic effect. MK is a pozzolan that develops its pozzolanic activity very fast and its effect can be observed from early ages of curing. At 3 days 100 % of the portlandite released by the cement was fixed; however, at 15 and 21 days of curing %CH was about 80 %, because the hydration of cement becomes more relevant than the pozzolanic reaction. The p-60FA presented a progressive increase of %CH over curing time, although more slowly than p-35MK. For longer curing ages such as 90 and 180 days all the portlandite released by the hydration reaction of cement was fixed by FA, therefore pozzolanic reactivity of FA took place later than MK. Despite the low reactivity of FA, the large proportion of this mineral addition and the low content of cement in this mixture, resulted in the total consumption of portlandite.

3.3 Scanning Electronic Microscopy (SEM)

Micrographs were taken by scanning electron microscopy to examine the hydration products formed in the different pastes tested after 28 days (Fig. 5)

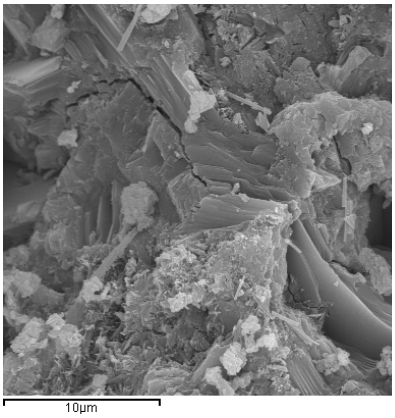

(a) p-OPC

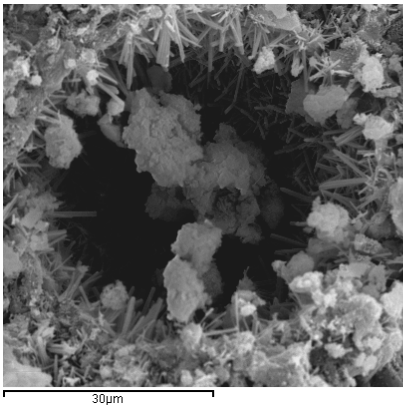

(b) p-OPC

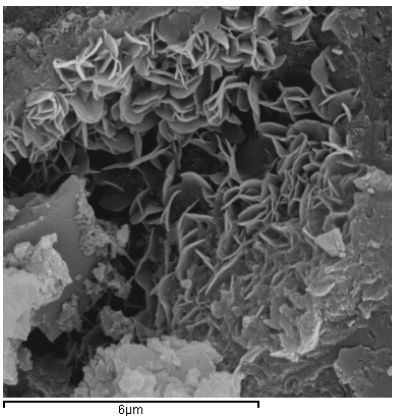

(c) p-35MK

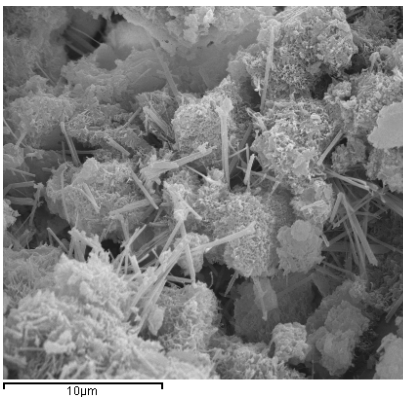

(d) p-35AN

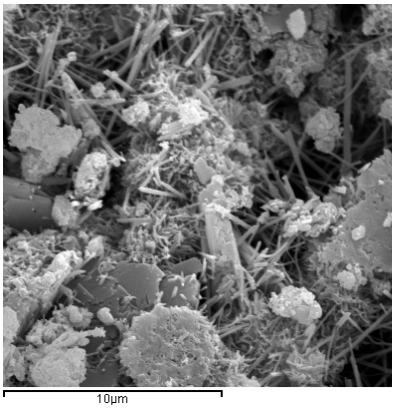

(e) p-60AN

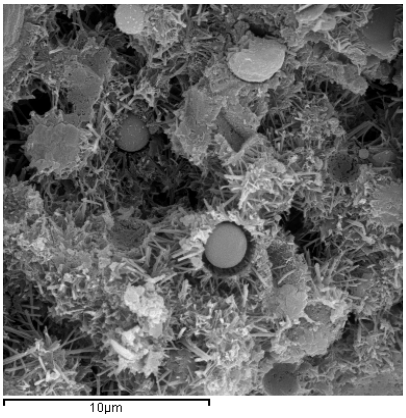

(f) p-60FA

1 *Fig. 5. Micrographs of p-OPC and blended pastes cured at 28 days.*

2

Micrograhs for p-OPC showed the typical presence of stacked portlandite (a), ettringite needles (b) and amorphous products were identified, mainly CSH in fibrillar appearance [31]. Paste p-35MK showed the typical crystals of hydrated gehlenite (c), attributed to the pozzolanic reaction. Pastes p-35AN (d) and p-60AN (e) had a more porous microstructure, the presence of portlandite and many particles (probably AN) were surrounded by hydration products. Finally, p-60FA showed many hydration products surrounding the spherical FA particles (f).

3.4 Mercury Intrusion Porosimetry (MIP)

Mortars were characterized by MIP after 360 days of curing. Fig. 6 (a) depicts cumulative intrusion volume curves obtained for the five types of mortars whose maximum value was related to the total porosity. The total porosity of m-OPC was 9.64 %, this value was the lowest because it had the greatest proportion of clinker. Mortars with 35 % and 60 % cement replacements by mineral admixture had a higher total porosity than m-OPC given their lower clinker content. Mortar m-35MK had a total porosity of 11.53 %, a value clearly lower than that presented by m-35AN (14.58 %), which indicates that there is a significant contribution of MK in reducing total porosity. Furthermore, the porosity of m-60FA was 16.86 %, which is lower than the corresponding value for m-60AN (19.97 %) thus these data

highlight the influence of FA in the development of the cementitious matrix.

The critical diameter (D_c) of pores corresponds to the highest slope in Fig 6 (a), and match with the highest peaks in Fig 6 (b). These values were 183 nm for m-60AN, 95 nm for m-35AN, 77 nm for m-OPC, 26 nm for m-60FA and 21 nm for m-35MK. It is remarkable that the mortars with pozzolans, which at 360 days had consumed all the portlandite, had higher total porosities than m-OPC, but the D_c was much smaller. The D_c value determines the pore size below which the mercury percolates through the sample. Pores with sizes below D_c constitute the connected porosity volume [32], and they are responsible for the electrical resistivity. The corresponding values of these connected porosity volumes for the tested mortars were: 4.01 % (m-OPC), 6.15 % (m-35AN), 8.27 % (m-60AN), 4.24 % (m-35MK) and 5.57 % (m-60FA).

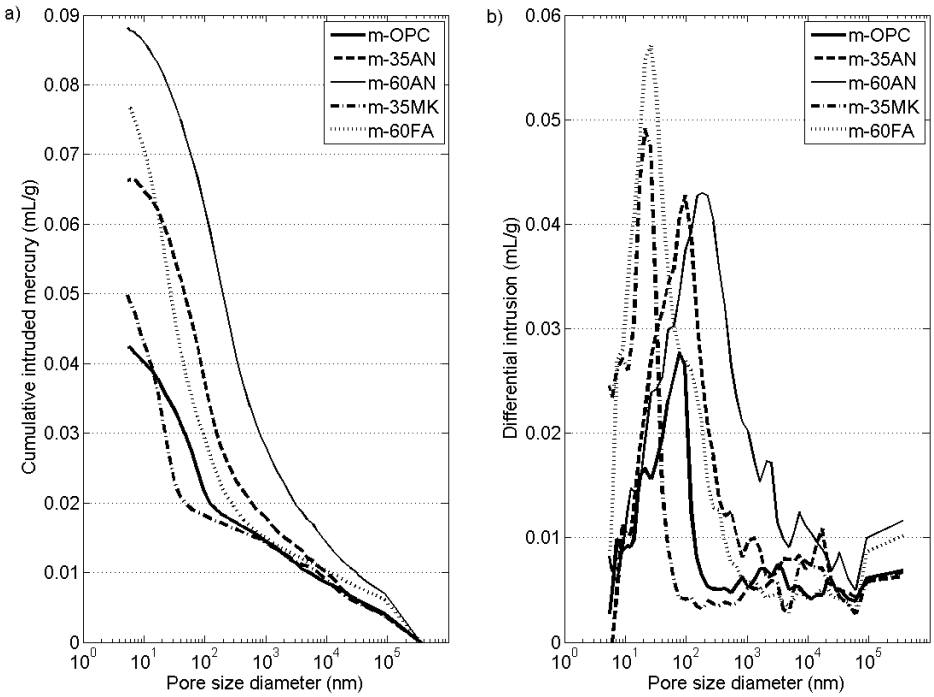

Fig. 6. (a) Cumulative intrusion of mercury volume curves for studied mortars. (b) Differential pore size distribution curves for studied mortars. Data measured at 360 days.

3.5 Electrical Impedance Measurements

3.5.1.- Equivalent electrical circuit (EEC)

The impedance data versus frequency were analyzed by EEC method [33, 34]. The main objective is to obtain an electrical circuit using a minimum

number of electrical components, with constant parameters, which have the same electrical impedance as the mortar in the frequency range tested in the experiment. If the same EEC is obtained throughout the hydration period, the changes of the electrical parameters can be used to assess the evolution of mortars and these parameters can also be linked to other microstructural measurements. The EEC shown in Fig. 7 was found to be very suitable for all mortars at any age of hydration.

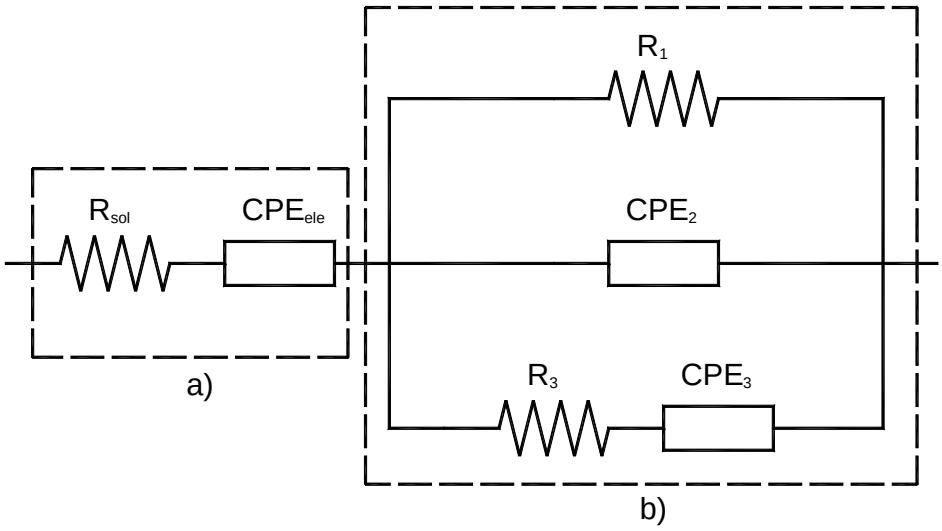

Fig. 7. Equivalent electrical circuit. The electrical components are resistors (R_{SOL}, R_1, R_3) and constant phase elements (CPE_{ele}, CPE_2 and CPE_3). The subcircuit (a) represents the impedance of the electrode-solution interface. The subcircuit (b) consists of three branches in parallel and represents the impedance of the mortar.

The parallel circuit with three branches has been used in several studies to explain the electrical behavior of cement mortars [19, 27, 35]. This circuit represents the three types of ionic conduction in the mortar. The resistance R_1 of the first branch represents the ionic conduction through the bulk solution into the connected pores of the capillary and/or gel porosity; it is in phase with the applied voltage and its admittance is frequency independent [35, 36]. The second and third branches have constant phase elements (CPE). The admittance of the CPE is:

$$Y(CPE)= Q\omega^{\alpha}\cos\alpha+j\cdot Q\omega^{\alpha}\text{sen}\alpha = Re(Y)+j\cdot Im(Y)$$

the Q-factor ($\Omega^{-1}s^{\alpha}rad^{-\alpha}$) and α-exponent (dimensionless, $0\leq\alpha\leq1$) are the two characteristic parameters of the CPE. The angular frequency is $\omega = 2\pi f$; f is the frequency of the applied voltage in Hz, and j = root (-1). Unlike the resistance, the admittance of a CPE has two components: the real part Re (Y) in phase with the applied voltage and the imaginary part Im (Y) lagged $\pi/2$ with applied voltage; both are frequency dependent [33].

The admittance of CPE_2 in the second branch represents the conductivity of a single phase in the mortar, probably related to the electrical double layer (EDL) formed at the solid-solution interface in the connected porosity, capillary and gel porosity of the C-S-H [37]. The third branch contains a resistor R_3 in series with a CPE_3, which represents the ionic conductivity along two different phases in series. This branch can be interpreted as the conductivity through the smallest pores of the C-S-H gel porosity, where the EDLs are overlapping and where the ionic transport is reduced [37]. R_3

represents the resistance through the solution of these nanopores and CPE_3 is related with the ion diffusion near the nanopore, where ions are accumulated and depleted [38].

The EEC was obtained by the free LEVM CNLS computer program [39]. The values of statistical parameters SF (relative standard deviation of the fit residuals) and PDRMS (root mean square value of the estimated relative standard deviations of the fit residuals) were less than 2 %, indicating that the proposed EEC yields a good fit [40]. In the two following subsections the electrical parameters of the EEC and its physical interpretation for all mortars are analyzed.

3.5.2. Ordinary Portland cement mortar (m-OPC) and blended mortars with an inert filler (m-35AN and m-60AN)

Fig. 8 illustrates the increase of R_1 with time of hydration for m-OPC, m-35AN and m-60AN from day 1 to 28.

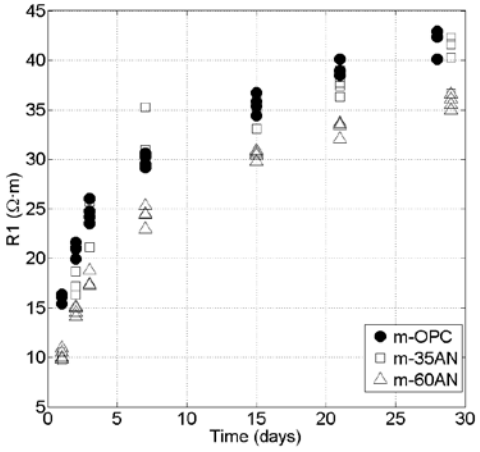

Fig. 8. R_1 versus time of hydration for the three mortars: m-OPC, m-35AN and m-60AN throughout the first 28 days of hydration.

The value of R_1 increased over time showing a decreasing slope. If the conductivity of the pore solution does not change significantly from the first day [41, 42], the increase in R_1 corresponds to a microstructural change in the connected porosity. To relate R_1 with the degree of hydration of cement, the Knudsen model can be applied [43]. According to this model, the hydration parameters vary over time following a parabolic expression. Applied to R_1, results the equation:

$$[(R_1/(R_{1max}-R_1)]^2 = a \cdot t + b \quad (1)$$

where R_{1max} is the asymptotic value of R_1; a and b are constants, and t is the time of hydration. The fitting of Eq. (1) in the first 28 days gave a maximum value for the determination coefficient $R^2 > 0.95$ with R_{1max} = 120 Ω·m for m-OPC, 115 Ω·m for m-35AN and 70 Ω·m for m-60AN. This good adjustment for R_1 with time leads us to consider R_1 as a parameter of

hydration, so the increase of R_1 is correlated with the interruption of the connected porosity through the hydration products, which reduce the pore diameter and increase the tortuosity of the path. The value of R_{1max} (120, 115, 70 ohmios·m) for m-OPC, m-35AN and m-60AN is inversely correlated with connected porosity volume (4.01%, 6.15%, 8.27%) and linearly correlated (R^2=0.995) with the critical diameter (77, 95, 183 nm) as calculated from the MIP measurements at the age of 365 days.

CPE_2 conductivity of the second branch is characterized by constant parameters Q_2 and α_2. Fig. 9 (a) shows the variation of α_2 over time. The exponent α_2 began with a value less than 0.40 for m-60AN, about 0.60 for m-35AN and about 0.70 for m-OPC, and increased clearly the first week. From day 14 the exponent α_2 reached a constant value close to 0.80 for all three mortars. This constant value of 0.80 was observed for cement paste in other studies in which an EEC of two parallel branches (R_1-CPE_2) was applied, and it was interpreted as a characteristic parameter of the fractality of pore size [44]. In another paper about mortars in which a two-branch EEC was applied, a value of α_2=0.7 was obtained, regardless of the w/c ratio [45]. In molecular sieve materials, values of α_2=0.51-0.66-0.81 were obtained, with pore sizes of 3.7-2.5-2.0 nm, respectively [46]. The obtained value α_2=0.8, clearly lower than 1, leads to the conclusion that CPE_2 is related to the ionic conductivity in the EDL of the pore surface [45].

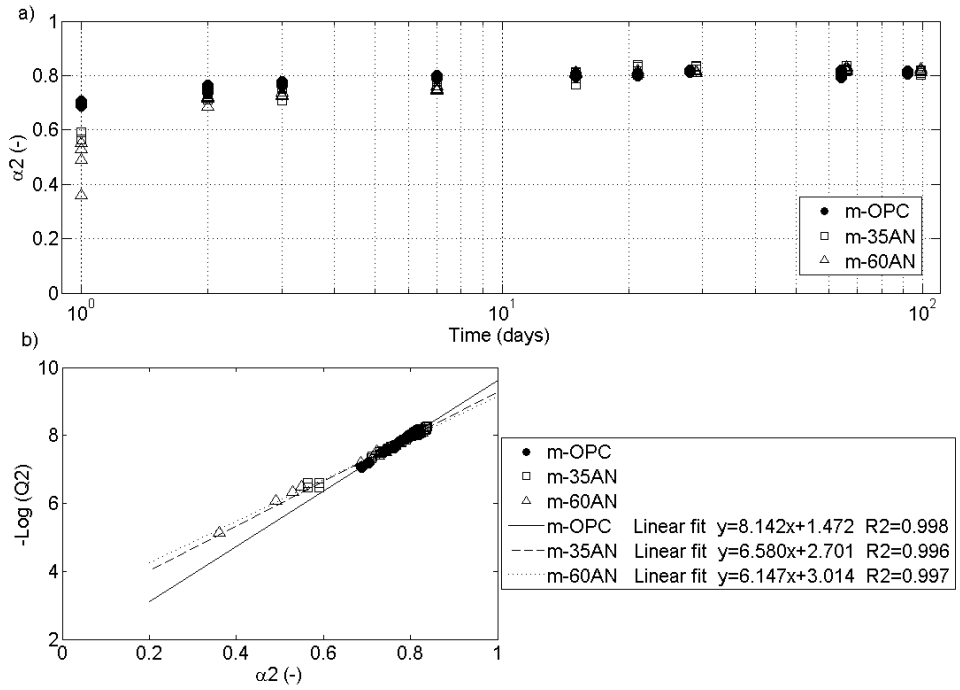

Fig. 9. (a) α_2 exponent of the CPE_2 in the second branch, for mortars m-OPC, m-35AN and m-60AN during the first 100 days (in log scale). (b) Plot of [-log (Q_2)] versus α_2 during the first 28 days of hydration, for all mortars (m-OPC, m-35AN and m-60AN). Regression straight lines and the coefficient of determination R^2 are shown.

The evolution of Q_2 over time behaved symmetrically with respect to α_2, the Q_2-factor decreased while the exponent α_2 increased, until reaching a threshold, minimum for Q_2 and maximum for α_2. Both saturation values were reached around day 14. Fig. 9 (b) shows the relationship between [-Log (Q_2)] and α_2 for the period 1 to 28 days. Linear fits were obtained with $R^2 > 0.99$ for the three mortars. It is observed that by increasing the

percentage of substitution with filler, the slope decreased while the independent term increased. This linear relationship has been found in random mixtures of two components, being one conductive and another dielectric, and α_2 the percentage of the dielectric component in the mixture [47, 48]. According to the Lichtenecker model [49], a logarithmic binary mixture consisting of a dielectric component with dielectric constant K, in proportion n, and a conductive component with conductivity S, in proportion (1-n), has a complex conductivity SC:

$$SC = S^{(1-n)} (j\omega K\varepsilon_0)^n = S^{(1-n)} (K\varepsilon_0)^n (j\omega)^n$$

being $\varepsilon_0 = 9.85 \cdot 10^{-12}$ (F/m) the dielectric permittivity of vacuum. This conductivity can be identified with a CPE, whose parameters are:

$$Q = S^{(1-n)} (K\varepsilon_0)^n = S \cdot (K\varepsilon_0/S)^n \quad (2a)$$

$$\alpha = n \quad (2b)$$

By taking logarithm of Q in eq (2a) it results:

$$Log(Q) = \alpha \cdot Log(K\varepsilon_0/S) + Log(S) \quad (3)$$

The electrical conductivity S (S/m = $\Omega^{-1} \cdot m^{-1}$) and the dielectric constant K (dimensionless) of the mixture were obtained by comparing eq. 3 with the experimental straight lines in Fig. 9 (b). This mixture could be identified as the hydrated product of the solid-liquid interface of the pores. For mortar m-OPC, S = 33.7 mS/m and K = 27.4, for m-35AN and m-60AN the conductivity decreased sharply until values of S = 2.0 and 1.0 mS/m, while K increased to values K = 59.2 and 77.9, respectively. According to this model, the three mortars reached the same proportion in the mixture of hydrated products at the interface, 80 % dielectric material and 20 %

conductive material, but by increasing the amount of filler, the conductive component became less conductive and the dielectric component became more insulating than m-OPC. Thus, CPE_2 in the second branch of the EEC is an electrical element with two parameters which allowed us to distinguish mortar with and without inert addition. Furthermore, the interpretation of CPE_2 as a dielectric-conductive mixture enforces the idea that CPE_2 represents the conductivity in the gel of hydrated products, located on the pore surface.

To relate directly the electrical parameters of the EEC to the degree of hydration of cement, R_1 and α_2 were compared with thermogravimetric parameters CH and H. For the three types of mortars, these parameters increased over time (see Table 3); their derivatives with respect to time were high up to 15 days, then decreased in the case of CH, and reached the saturation (derivatives = 0) for H. R_1 and α_2 behaved similarly. The best linear fits of R_1 and α_2 were obtained with respect to CH. Relationships are depicted in Fig. 10 (a) and (b).

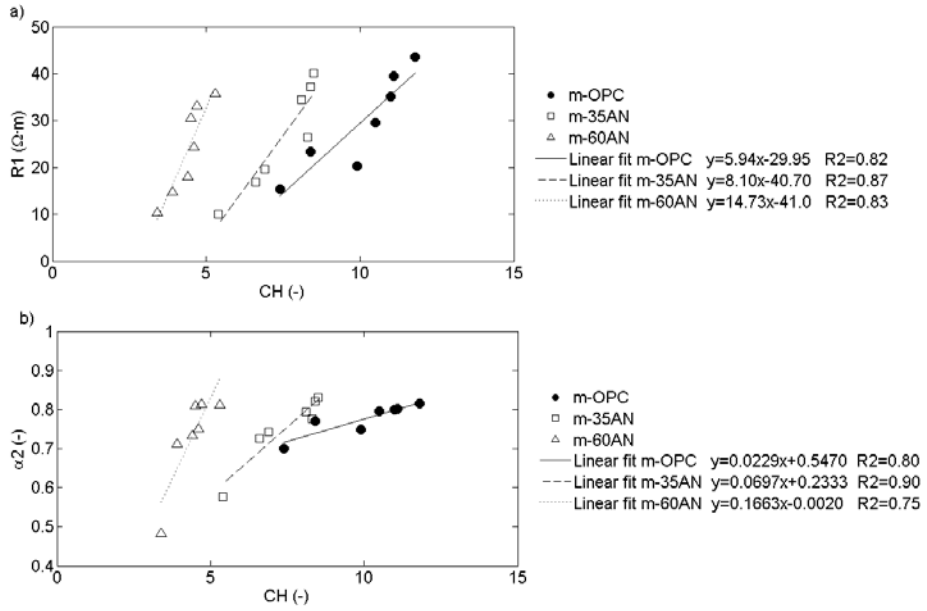

Fig. 10. (a) Mean value of electrical resistance R_1 versus the content of portlandite (CH, % w) for the three mortars (m-OPC, m-35AN and m-60AN) during the first 28 days of hydration. (b) Mean value of exponent α_2 of CPE_2 versus CH for the three mortars (m-OPC, m-35AN and m-60AN). The straight lines of regression and the determination coefficient R^2 are shown.

A linear relationship between CH and the electrical resistance R_1 for the three mortars is observed with a determination coefficient R^2= 0.82 - 0.87. Mortar m-OPC showed the highest content of portlandite as well as the highest value of R_1. The slopes of straight lines increased as the amount of cement decreased, which indicates that CH was more effective for increasing the resistance R_1 in this order: m-60AN > m-35AN > m-OPC.

Furthermore, the same value of R_1 was achieved with different values of CH in each mortar, and with the same quantity of portlandite, the m-35AN reached a higher value for R_1 than did m-OPC. This means that other factors, not directly related to the amount of hydration products, are involved in R_1. A similar analysis was done with the exponent α_2. The α_2 exponent increased up to 14 days, then it saturated. This behavior was similar to those of CH and H. The best correlation was found between α_2 and CH. Fig. 10 (b) shows the linear relationship; the values of R^2 are similar to those of R_1, and it also shows that the slope of increase of α_2 with CH is higher for m-60AN and lower for m-OPC. Therefore, the parameters R_1 and α_2 are directly related to CH.

The third branch of the EEC contains a resistor R_3 in series with an electrical CPE_3. The values obtained for α_3 were about 0.50 for the three mortars over the full hydration period. The value $\alpha = 0.5$ in a CPE has been related to the ion diffusion phenomena that occur in small size constrictions or defects [50]. This value supports the idea of a third branch which accounts for the conductivity in the smallest pores of the CSH gel (<10 nanometers). R_3 began with values about 500 Ω·m and increased to values between 2000 and 3000 Ω·m on 100 days for all three mortars. This behavior indicates that the pore size constraints were still increasing and the hydration process continued up to 3 months.

3.5.3. Blended mortars with pozzolans (m-60FA and m-35MK)

Fig. 11 shows the evolution of R_1 over time for m-60FA and m-35MK, m-OPC is included as reference.

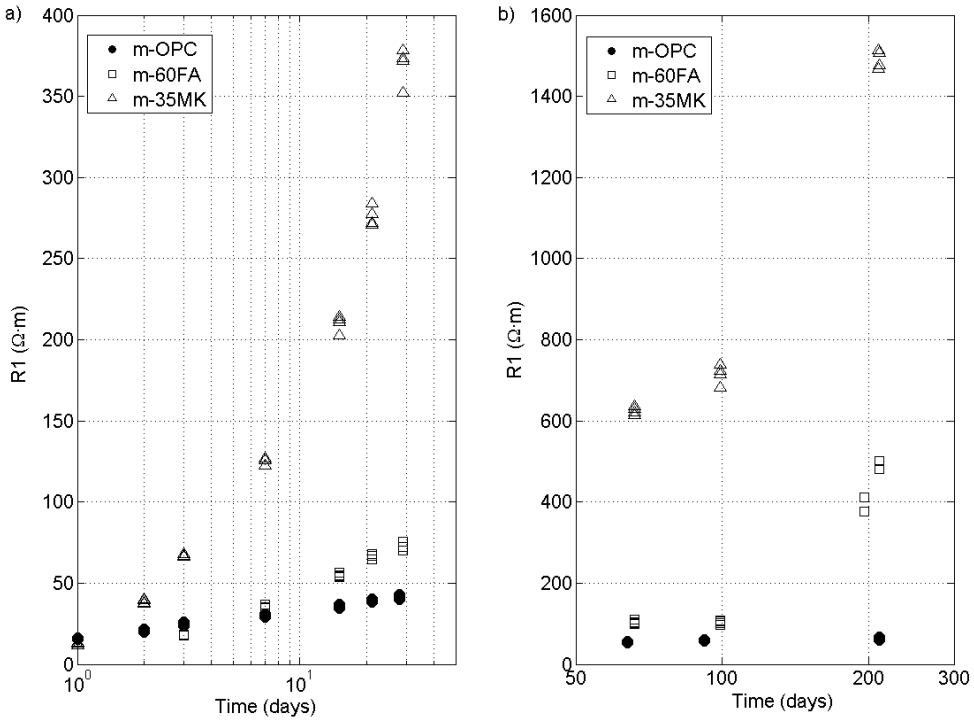

Fig. 11. R_1 value of the EEC versus curing time (log scale) for the three mortars (m-OPC, m-60FA and m-35MK). (a) From 1 to 28 days, (b) from 50 to 212 days.

R_1 for pozzolanic mortars m-60FA and m-35MK were larger than m-OPC throughout the hydration period, except for the first day in the case of m-35MK and for the first week in the case of m-60FA. R_1 of m-60FA followed the Knudsen hydration model, over the first 28 days with R_{1max} = 300 Ω·m, while R_1 of m-35MK did not. At day 28 R_1 of m-60FA was two times the value of m-OPC, while the value of m-35MK was seven times. The effect of pozzolanic replacements on the evolution of R_1 was quite different. On day 200 the values of R_1 for blended mortars were much higher than in the first 100 days. Between days 100 and 200, R_1 was multiplied by a factor of 2 for m-35MK (1500 Ω·m) and by a factor of 4 (400 Ω·m) for m-60FA. The largest increase in R_1 for m-60FA between 100 and 200 days, coincided with the complete consumption of portlandite at day 90. The final R_1 value and how it changed over time were the two great differences between pozzolanic mortars of FA and MK.

Fig. 12 (a) shows the exponent α_2 of the CPE_2 of the second branch for the three mortars. The α_2 exponent followed the same trend for m-OPC and m-35MK during the first 28 days. Both started with values between 0.60 and 0.70 and then they increased in the first week until reaching limit values of 0.80 (m-OPC) and 0.75 (m-35MK). Around day 200, m-35MK reached a high value of 0.9. Exponent α_2 of m-60FA started about 0.70 and continued with values between 0.60 and 0.70 until day 200.

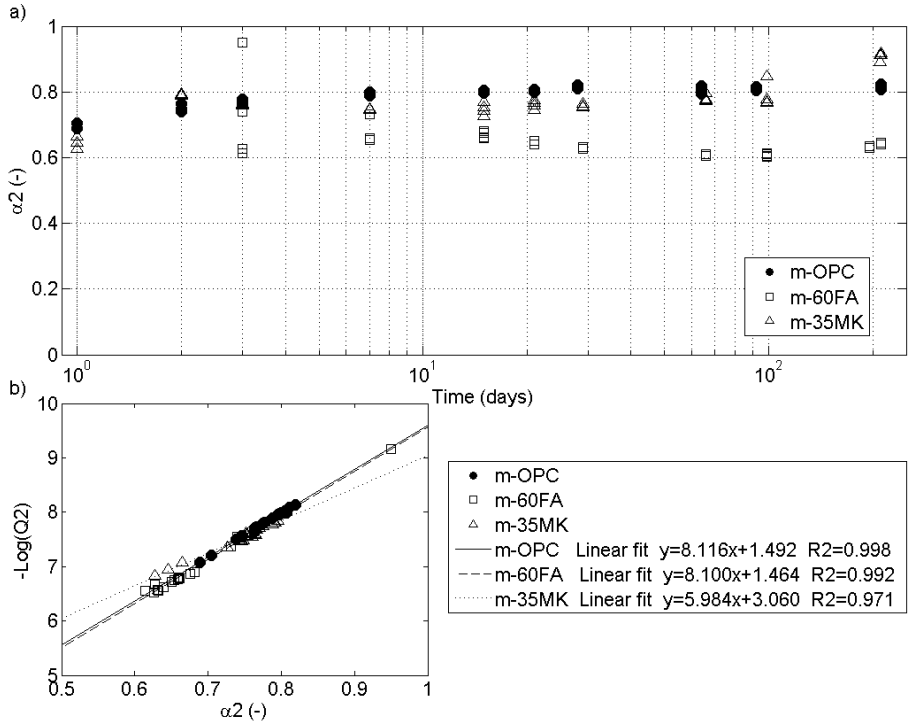

Fig. 12. (a) CPE exponent α_2 of the second branch for mortars (m-OPC, m-35MK and m-60FA) (in log scale). (b) -Log (Q_2) versus α_2 for all mortars (m-OPC, m-35MK and m-60FA) in the period 1-28 days of hydration. The straight lines of regression and the determination coefficient R^2 are shown.

These data indicate that the two pozzolans produced a mixture of hydration products at the interface in different proportions. The material of the pore-solution interface of m-OPC had an 80 % dielectric component until day 200, while m-35MK had 75 % until day 100 but it reached 90 % on day 200. By contrast, m-60FA had throughout the hydration period a lower

proportion of dielectric component, 60 to 70 %. Fig. 12 (b) depicts the relationship between [-Log (Q_2)] and α_2 for the period 1-28 days. Linear relations were obtained with good fits in all mortars, with $R^2 > 0.97$. Linear equations in m-OPC and m-60FA had similar coefficients, but they were different for m-35MK. Applying the same logarithmic mixing model as before (eq. 3) to interpret the mixture of the interface, m-60FA had values of S = 34.4 mS/m and K = 30.9, which were similar to m-OPC (32.2 mS/m and 27.9). In m-35MK, the S value decreased to 0.9 mS/m, and the value of K increased to 102. The difference between m-OPC and m-60FA was in the dielectric percentage, 80 % for m-OPC and between 60% and 70 % for m-60FA. Mortar m-35MK had the lowest value of S, in the same order of magnitude as the filler mortars, m-35AN (2 mS/m) and m-60AN (1 mS/m) but a value of K = 102 which was much higher than those of the inert addition mortars (59.2 and 77.9, respectively). Just as happens in mortars with filler, the parameters of CPE_2 also allow us to characterize different pozzolanic mortars.

The parameters of the third branch for m-35MK and m-60FA had different values and behaved differently with respect to m-OPC. In mortars with pozzolans, α_3 was different from 0.5 which was the value obtained for m-OPC, m-35AN and m-60AN in the first 100 days. Mortar m-35MK had very high values for α_3 the first few days, reaching the maximum value of 1 and then decreasing over time, approaching to 0.6 at the end of the

hydration period. Mortar m-60FA had a value close to 0.6 throughout nearly the entire hydration period and a value of 0.5 at the end.

4 CONCLUSIONS

1. Mixtures containing MK and FA in large cement replacement levels (35 and 60 %, respectively) yielded cementing matrices without portlandite, from 3 days and 3 month of hydration, respectively.
2. Total porosities of mortars containing high percentages of MK and FA were higher than those obtained for plain OPC, whereas the critical diameter was considerably reduced (pore refinement) due to the pozzolanic reaction.
3. The procedure of variable area for measurement was useful to obtain the mortar impedance that can be analyzed satisfactorily with the same EEC for all mortars and hydration ages.
4. The three-branch ECC which represents the three different types of ionic conductivity in the mortar fits accurately to the impedance data.
5. R_1 is related to the degree of hydration and it allows us to characterize plain mortar, inert filler mortar and pozzolan mortars.
6. CPE_2 quantifies the electrical properties of the hydration products located at the solid-solution interface. It also allows us to

characterize the different mortars, with filler and pozzolan, and even distinguish the type of pozzolan.

ACKNOWLEDGEMENTS

The authors thank the *Universitat Politècnica de València* (*UPV, Vicerrectorado de Investigación*) for its support (project PAID-05-09 ref 4302) and Debra Westall (UPV) for revising the manuscript.

REFERENCES

[1] V.M. Malhotra, P.K. Mehta, Pozzolanic and cementitious materials, Gordon and Breach Publishers, Ottawa, 1996.

[2] R. Roskovic, D. Bjegovic, Role of mineral additions in reducing CO_2 emission, Cem. Concr. Res. 35 (2005) 974-978.

[3] F. Massazza, Pozzolana and pozzolanic cements, in: Hewlett PC (ed) Lea's chemistry of cement and concrete, fourth ed. Elsevier, UK, 2007, pp. 471–602.

[4] S. Caijun, Studies on several factors affecting hydration and properties of portlandite-pozzolan cements, J. Mater. Civ. Eng. 13 (2001) 441–445.

[5] J. Payá, J. Monzó, V. Borrachero, E. Peris, E. González, Mechanical

treatments of fly ashes. Part III: Studies on strength development of ground fly ashes (GFA)- cement mortars, Cem. Concr. Res. 27 (1997) 1365-1377.
[6] R.F. Feldman, H. Cheng-Yi, Microstructure properties of blended cement mortars and their relation to durability, Proceedings of the RILEM Seminar on Durability of Concrete Structures under Normal Outdoor Exposure, Hannover, March, 1984, pp. 133–140.
[7] L. Lam, Y.L.Wong, C.S. Poon, Degree of hydration and gel/space ratio of high-volume fly ash/cement systems, Cem. Concr. Res. 30 (2000) 747–756.
[8] P.K. Metha, High-performance, high-volume fly ash concrete for sustainable development, Proceedings of the International Workshop on Sustainable Development and Concrete Technology, Beijing, 2004, pp. 3–14.
[9] P.C. Aitcin, High Performance Concrete, E& FN SPON, London, 1998.
[10] M. Cyr, P. Lawrence, E. Ringot, Efficiency of mineral admixtures in mortars: quantification of the physical and chemical effects of fine admixtures in relation with compressive strength, Cem. Concr. Res. 36 (2006) 264–277.
[11] A. Xu, S.L. Sakar, L.O. Nilsson, Effect of fly ash on the micro-structure of cement mortar, Mater. Struct. 26 (1993) 414–424.
[12] V.G. Papadakis, Effect of fly ash on Portland cement systems, Part I. Low-calcium fly ash, Cem. Concr. Res. 29 (1999) 1727–1736.
[13] E.E. Berrey, R.T. Hemmings, B.J. Cornelius, Mechanisms of hydration reaction in high volume fly ash cements and mortars, Cem. Concr. Compos. 12 (1990) 253–261.

[14] Instrucción para el hormigón estructural EHE08, Real decreto 1429/2008, Spain, 2008

[15] G. Kakali, T. Perraki, S. Tsivilis, E. Badogiannis, Thermal treatment of kaolin: the effect of mineralogy on the pozzolanic activity. Appl. Clay Sci. 20 (2001) 73-80.

[16] B.B. Sabir, S. Wild, J. Bai, Metakaolin and calcined clays as pozzolans for concrete: a review, Cem. Concr. Compos. 23 (2001) 441-454.

[17] R. Siddique, J. Klaus, Influence of metakaolin on the properties of mortar and concrete: A review, Appl. Clay Sci. 43 (2009) 392–400.

[18] K.A. Snyder, D. P. Bentz, Suspended hydration and loss of freezable water in cement pastes exposed to 90% relative humidity, Cem. Concr. Res. 34 (2004) 2045-2056.

[19] M. Cabeza, M. Keddam, X.R. Novoa, I. Sánchez, H. Takenouti, Impedance spectroscopy to characterize the pore structure during the hardening process of Portland cement paste, Electrochim. Acta 51 (2006) 1831-1841.

[20] S. Diamond, Mercury porosimetry: an inappropriate method for the measurement of pore size distributions in cement-based materials, Cem. Concr. Res. 30 (2000) 1517–1525.

[21] M.C.G. Juenger, H.M. Jennings, The use of nitrogen adsorption to assess the microstructure of cement paste, Cem. Concr. Res. 31 (2001) 883–892.

[22] Q. Zeng , K. Li, T. Fen-chong, P. Dangla, Pore structure characterization of cement pastes blended with high-volume fly-ash, Cem. Concr. Res. 42 (2012) 194–204.

[23] E. Güneyisi, M. Gesoglu, K. Mermerdas, Improving strength, drying shrinkage, and pore structure of concrete using metakaolin, Mater. Struct. 41 (2008) 937-949.

[24] S. Wansom, S. Janjaturaphan, S. Sinthupinyo, Characterizing pozzolanic activity of rice husk ash by impedance spectroscopy, Cem. Concr. Res. 40 (2010) 1714-1722.

[25] J.M. Cruz, J. Payá, L.F. Lalinde, I. Fita, Evaluation of electric properties of cement mortars containing pozzolans, Materiales Constr. 61 (2011) 7-26.

[26] K. A. Snyder, The relationship between the formation factor and the diffusion coefficient of porous materials saturated with concentrated electrolytes: theoretical and experimental considerations, Concr. Sci. Eng. 3 (2001) 216-224.

[27] M. Cabeza, P. Merino, A. Miranda, X. R. Novoa, I. Sánchez, Impedance spectroscopy study of hardened Portland cement paste, Cem. Concr. Res. 32 (2002) 881-891.

[28] X. Ji, S.Y.N. Chan, N. Feng, Fractal model for simulating the space-filling process of cement hydrates and fractal dimensions of pore structure of cement-based materials, Cem. Concr. Res. 27 (1997) 1691-1699.

[29] G. Vagelis, G. Papadakisa, Effect of fly ash on portland, cement systems: Part I. Low-calcium fly ash, Cem. Concr. Res. 29 (1999) 1727-1736.

[30] J. Payá, J. Monzó, M.V. Borrachero, S. Velázquez, Evaluation of the pozzolanic activity of fluid catalytic cracking catalyst residue (FC3R). Thermogravimetric analysis studies on FC3R-Portland cement pastes, Cem.

Concr. Res. 33 (2003) 603-609.

[31] K.L. Scrivener, A. Nonat, Hydration of cementitious materials, present and future, Cem. Concr. Res. 41 (2011) 651-665.

[32] A.J. Katz, A. H. Thomson, Prediction of rock electrical conductivity from Mercury injection measurements, J. Geophys. Res. 92 (1987) 599-607.

[33] J.R. MacDonald, Impedance Spectroscopy, Wiley, New York, 1987.

[34] W.J. McCarter, G. Starrs, T.M. Chrisp, Electrical conductivity, diffusion, and permeability of Portland cement-based mortars, Cem. Concr. Res. 30 (2000) 1395-1400.

[35] B. Díaz, L. Freire, P. Merino, X.R. Novoa, M.C. Pérez, Impedance spectroscopy study of saturated mortar samples, Electrochim. Acta 53 (2008) 7549-7555.

[36] D.E. Macphee, D.C. Sinclair, S.I. Cormack, Development of an equivalent circuit model for cement pastes from microstructural considerations, J. Am. Ceram. Soc. 80 (1997) 2876-2884.

[37] Y. Elakneswaran, A. Iwasa, T. Nawa, T. Sato, K. Kurumisawa, Ion-cement hydrate interactions govern multi-ionic transport model for cementitious materials, Cem. Concr. Res. 40 (2010) 1756-1765.

[38] R. Dhopeshwarkar, R.M. Crooks, D. Hlushkou, U. Tallarek, Transient effects of microchannel electrokinetic filtering with an ion-permselective membrane, Anal. Chem. 80 (2008) 1039-1048.

[39] J.R. Macdonald, Comparison of parametric and nonparametricmethods for the analysis and inversion of immittance data: Critique of Earlier Work, J.Comput. Phys. 157 (2000) 280-301.

[40] J.R. McDonald, Utility of continuum diffusion models for analyzing mobile-ion inmittance-data: electrode polarization, bulk, and generation-recombination effects, J. Phys. Condens. Mater. 22 (2010) doi: 10.1088/0953-8984/22/49/495101.

[41] M.R. Nokken and R.D. Hooton, Using pore parameters to estimate permeability on conductivity of concrete, Mater. Struct. 41 (2008) 1-16.

[42] X. Wei and Z. Li, Study of Portland cement with fly ash using electrical measurement, Mater. Struct. 38 (2005) 411-417.

[43] D.P. Bentz, Three-dimensional computer simulation of portland cement hydration and microstructure development, J. Am. Ceram. Soc. 80 (1997) 3-21.

[44] S.S. Yoon, H.C. Kim, R.M. Hill, The dielectric response of hydrating porous cement paste, J. Phys. D: Appl. Phys. 29 (1996) 869-875.

[45] A. Berg, G.A. Niklasson, K. Brantervik, B. Hedberg, L.O. Nilsson, Dielectric properties of cement mortar as a function of water content, J. Appl. Phys. 71 (1992) 5897-5903.

[46] M. Kinka, J. Banys, J. Makutkevic, A. Meskauskas, Conductivity of nanostructured mesoporous MCM-41 molecules sieve materials, Electrochim. Acta 51 (2006) 6203-6206.

[47] D.P. Almond, B. Vainas, The dielectric properties of random R-C networks as an explanation of the “universal” power law dielectric response of solids, J. Phys. Condens. Matter. 11 (1999) 9081-9093.

[48] C.R. Bowen, A.C.E. Dent, D.P. Almond, T.P. Comyn, Modelling power law dependencies of frequency dependent AC conductivity and permittivity of conductor-relaxor composites, Ferroelectrics 370 (2008) 166-175.

[49] T. Zakri, J.P. Laurent, M. Vauclin, Theoretical evidence for Lichtenecker mixture formulae based on the effective medium theory, J. Phys. D: Appl. Phys. 31 (1998) 1589-1594.

[50] G. Valincius, T. Meskauskas, F. Ivanauskas, Electrochemical impedance spectroscopy of tethered bilayer membranes, Langmuir 28 (2012) 977-990.

Figure captions

Fig. 1. Particle size distribution of mineral additions (relative frequency is measured in % by volume).

Fig. 2. a) Compressive strength values versus curing time for all mortars; b) SAI values of mortars versus curing time (3, 7, 15, 28, 180 days, in log scale).

Fig. 3. DTG curves for pastes cured at 28 days (a) and 180 days (b). (The curves are separated in order to better observe the peak values.

Fig. 4. Percentage of portlandite fixation versus curing time (log scale) for cement pastes with mineral additions.

Fig. 5. Micrographs of p-OPC and blended pastes cured at 28 days.

Fig. 6. (a) Cumulative intrusion of mercury volume curves for studied mortars. (b) Differential pore size distribution curves for studied mortars. Data measured at 360 days.

Fig. 7. Equivalent electrical circuit. The electrical components are resistors (R_{SOL}, R_1, R_3) and constant phase elements (CPE_{ele}, CPE_2 and CPE_3). The subcircuit (a) represents the impedance of the electrode-solution interface. The subcircuit (b) consists of three branches in parallel and represents the impedance of the mortar.

Fig. 8. R_1 versus time of hydration for the three mortars: m-OPC, m-35AN and m-60AN throughout the first 28 days of hydration.

Fig. 9. (a) α_2 exponent of the CPE_2 in the second branch, for mortars m-OPC, m-35AN and m-60AN during the first 100 days (in log scale). (b) Plot of [-log (Q_2)] versus α_2 during the first 28 days of hydration, for all mortars (m-OPC, m-35AN and m-60AN). Regression straight lines and the coefficient of determination R^2 are shown.

Fig. 10. (a) Mean value of electrical resistance R_1 versus the content of portlandite (CH, % w) for the three mortars (m-OPC, m-35AN and m-60AN) during the first 28 days of hydration. (b) Mean value of exponent α_2

of CPE_2 versus CH for the three mortars (m-OPC, m-35AN and m-60AN). The straight lines of regression and the determination coefficient R^2 are shown.

Fig. 11. R_1 value of the EEC versus curing time (log scale) for the three mortars (m-OPC, m-60FA and m-35MK). (a) From 1 to 28 days, (b) from 50 to 212 days.

Fig. 12. (a) CPE exponent α_2 of the second branch for mortars (m-OPC, m-35MK and m-60FA) (in log scale). (b) -Log (Q_2) versus α_2 for all mortars (m-OPC, m-35MK and m-60FA) in the period 1-28 days of hydration. The straight lines of regression and the determination coefficient R^2 are shown.